buildings

MDPI

Article

Evaluation Method and Influence Law of UV-Cured Polyurethane on the Self-Healing Performance of Asphalt and Asphalt Mixtures

Huaizhang Sun [1], Wenyi Liu [1], Yu Wang [1], Xinyue Chang [2], Hu Zhao [1], Shengkang Shi [1], Jianbao Xing [3], Di Wu [3], Jizhe Zhang [4] and Wengang Zhang [5,*]

1 Tianjin South Railway Station Technology Business District Development Co., Ltd., Tianjin 300380, China; wangyunzswq@163.com (Y.W.)
2 Tianjin Engineering & Construction Corporation, Tianjin 300384, China
3 Haiwei Engineering Construction Co., Ltd. of FHEC of CCCC, Beijing 101119, China; xingjianbao1004@126.com (J.X.)
4 School of Qilu Transportation, Shandong University, Jinan 250061, China
5 School of Civil Engineering and Geomatics, Shandong University of Technology, Zibo 255049, China
* Correspondence: ziwuzizwg@sdut.edu.cn

Abstract: To explore the effect of UV-curable polyurethane (UV-PU) on the self-healing performance (SHP) of asphalt and asphalt mixtures, this article conducted research in this area of the evaluation method and influenced the law. polyurethane (PU), Styrene-Butadiene-Styrene Block Copolymer (SBS I-C) and 70# asphalt and asphalt mixtures were introduced as the example of comparison. A method for evaluating the SHP of asphalt, sand asphalt mixture, and medium particle asphalt mixture using the healing index (HI) as an evaluation index was proposed, and the healing performance of various materials under different healing conditions was tested and analyzed. The research results indicate that, HI based on asphalt complex shear modulus (HI_A), HI based on sand type asphalt mixture (AC-5) flexural tensile strength ($HI_{AC\text{-}5}$), and HI based on medium grained asphalt mixture (AC-16) bending stiffness modulus (S) $HI_{AC\text{-}16}$ can effectively reflect the SHP of asphalt, AC-5, and AC-16 under different healing conditions, and can be used as an evaluation indicator for SHP. The asphalt SHP is related to the asphalt type and the degree of initial loss and is highly correlated with the healing time. Compared to other asphalt types, the sensitivity of UV-PU or PU modified asphalt to initial loss is lower than that of SBS I-C modified asphalt, but higher than 70# asphalt. Under the same light healing time and initial degree of loss, the SHP of UV-PU modified asphalt AC-5 and AC-16 is significantly superior to other types of asphalt mixtures. Compared to asphalt, the self-healing time of AC-5 grade AC-16 is longer. The SHP of AC-16 is highly correlated with the loss degree associated with the initial S. The larger the initial loss degree of the S, the greater the loss rate of the HI.

Keywords: UV-PU modified asphalt; self-healing performance; healing index; complex shear modulus; bending stiffness modulus

check for updates

Citation: Sun, H.; Liu, W.; Wang, Y.; Chang, X.; Zhao, H.; Shi, S.; Xing, J.; Wu, D.; Zhang, J.; Zhang, W. Evaluation Method and Influence Law of UV-Cured Polyurethane on the Self-Healing Performance of Asphalt and Asphalt Mixtures. *Buildings* **2023**, *13*, 1277. https://doi.org/10.3390/buildings13051277

Academic Editor: Elena Ferretti

Received: 25 April 2023
Revised: 6 May 2023
Accepted: 12 May 2023
Published: 14 May 2023

Copyright: © 2023 by the authors. Licensee MDPI, Basel, Switzerland. This article is an open access article distributed under the terms and conditions of the Creative Commons Attribution (CC BY) license (https://creativecommons.org/licenses/by/4.0/).

1. Introduction

Crack disease is a common types of asphalt pavement disease. The self-healing technology for road surface cracks is mainly divided into two types: active self-healing and passive self-healing [1]. Active self-healing generally increases temperature by adding conductive particles to the binder and using induction energy and locally heating asphalt concrete to improve its performance. Passive self-healing generally involves embedding microcapsules containing chemicals in the binder. When micro cracks begin to appear in the binder, they can cause loss to the capsule, causing the chemicals to diffuse into the binder, thereby repairing the material and improving the healing rate of asphalt [2]. Scholars have also proposed the concept of automatic healing [3–5]. Aasphalt and asphalt mixture have

a certain SHP under certain temperature and time conditions. However, how to improve SHP has become a challenge for road workers [6–8].

Polyurethane (PU) is a polymer containing repeated carbamate groups in the molecular chain segment. Carbamate is usually obtained by the reaction of isocyanate and alcohol, and polyurea is obtained by the reaction of a polyisocyanate polyamine is also a polyurethane material in a broad sense [9–12]. PU resin has a series of excellent properties. It is a thermosetting resin that can greatly improve the pavement performance of asphalt [13]. Moreover, PU can react with various compounds, which helping to reduce the segregation of SBS. UV-curable polyurethane (UV-PU) materials utilize the photosensitivity of UV initiators (photosensitizers) to form excited ecological molecules under UV light irradiation, decompose into free radicals or ions, and undergo chemical reactions such as polymerization, grafting, and crosslinking of unsaturated organic compounds in polyurethane materials to achieve curing [14–18]. UV curing technology is widely used in the field of UV-PU coatings. Research has shown that UV-PU coatings have excellent self-healing properties [19–22]. With the gradual application promotion of UV-curable polyurethane in asphalt, its improvement in SHP of asphalt has gradually attracted the attention of industry professionals [23,24]. Research has shown that UV-curable polyurethane is a polyurethane containing exocyclic butane substituted chitosan groups [25,26]. Under the action of UV light, its internal chitosan ring will open and generate free radicals, which can bond with the free radicals generated during loss to achieve self-healing [27–30]. However, there are few effective references available, which has caused certain difficulties for research in this field.

In short, there are still several unresolved issues in the research field.

(1) Lack of evaluation methods and indicators for the SHP.
(2) The effect of UV-PU on the SHP is not yet clear.
(3) The influencing factors and patterns of the SHP of UV-PU modified asphalt and asphalt mixtures are not yet clear enough.

Based on the above background, to explore the effect of UV-PU on the SHP, this article conducted research in this area of the evaluation method and influenced the law. PU, SBS I-C and 70# asphalt and asphalt mixtures were introduced as the example of comparison. A method for evaluating the SHP of asphalt, sand asphalt mixture, and medium particle asphalt mixture using the HI as an evaluation index was proposed. HI based on asphalt complex shear modulus (HI_A), HI based on sand type asphalt mixture (AC-5) flexural tensile strength ($HI_{AC\text{-}5}$), and HI based on medium grained asphalt mixture (AC-16) bending stiffness modulus (S) $HI_{AC\text{-}16}$ were used to reflect the SHP of asphalt, AC-5, and AC-16 under different healing conditions.

2. Materials and Methods

2.1. Materials

PU and UV-PU are provided by Zibo Hengjing PU Technology Co., Ltd. (Zibo, China). The technical specifications of polyurethane are shown in Table 1, and the technical specifications of UV-PU are shown in Table 2. Asphalt is provided by Shandong Expressway Group (Jinan, China), and the technical indicators are shown in Table 3. The aggregates are provided by Shandong Jiuqiang Group (Zibo, China), and the technical indicators are shown in Table 4.

The preparation process of PU modified asphalt and UV-PU modified asphalt is as follows: a certain amount of modifier is added to asphalt at 145 °C, cut at a shear rate of 1500 r/min for 30 min. Then the temperature is raised to 175 °C, and the asphalt is cut at a rate of 5000 r/min for 45 min to obtain PU modified asphalt or UV-PU modified asphalt. In this paper, the content of PU or UV-PU is both 5% of the mass of asphalt. Figure 1 shows the preparation process.

Table 1. Technical performance of PU.

Technical Performance	Measured Value	Test Method
NCO content, %	5.9	ASTM D5155
85 °C Viscosity, MPa · s	958	ASTM D4889
Gelation time, min	6.8	GB/T 24148.7-2014
Hardness, Shore A	96.3	GB/T 531-1999
Tensile strength, MPa	58	GB/T 528-2009
Rebound, %	23	GB/T 1681-2009
Density, g/cm^3	1.27	ASTM D891
20 °C State of matter	white solid	

Table 2. Technical performance of UV-PU.

Technical Performance	Measured Value	Test Method
Hardness, Shore A	55.3	GB/T 531-1999
Tensile strength, MPa	2.47	GB/T 528-2009
Elongation at break, mm · mm$^-$	3.24	GB/T 528-2009
Breaking strength, MPa · s	5.78	GB/T 529-2008

Table 3. Technical performance of asphalt.

Testing Items		70#	SBS I-C
Penetration at 25 °C, 0.1 mm		74.2	68.8
Ductility at 5 °C, cm		——	45.6
Softening point at, °C		47.5	72.3
Ductility at 10 °C, cm		29.7	——
RTFOT [1]	Mass change, %	−0.2	0.1
	Residual ductility at 10 °C, %	15.8	——
	Residual ductility at 5 °C, %	——	28.3
	Residual penetration ratio at 25 °C, %	71.7	76.2

[1] RTFOT: Rotating thin film heating test.

Table 4. Technical performance of aggregates.

Aggregate Type	Technical Indicators	Measured Value
Fine aggregate	Soundness, %	7.8
	Sand equivalent, %	72.7
	Mud content, %	1.2
	Methylene blue value, g/kg	14.3
	Angularity, s	18.1
Coarse aggregate	Los Angeles abrasion loss, %	8.2
	Crushing value, %	10.1
	Water absorption, %	0.44
	Needle and flaky content, %	5.5
	Soundness, %	7.3

2.2. Evaluation Method and Test Design for SHP

2.2.1. Evaluation Method and Test Design of Asphalt SHP

The 70# asphalt and PU or UV-PU were used to prepare the PU or UV-PU modified asphalt, the time scanning was performed on the asphalt using a dynamic shear rheometer (DSR). The control mode was strain control, with a loading frequency of 10 Hz, strain control of 10%, the thickness of asphalt was 2 mm, and loading temperature is 20 °C. The test was conducted by loading, healing, and loading methods. When the loss values of the asphalt complex modulus (G*) reached 20%, 40%, and 60%, the loading was stopped. Then, the asphalt was given healing times of 10, 20, and 30 min, respectively. G* was tested

separately, as shown in Figure 2, the healing status was evaluated according to Equation (1). The same test also applies to SBS I-C and 70# asphalt.

$$HI_A = \frac{G^*_{2-i-j} - G^*_{1-i}}{G^*_0 - G^*_{1-i}} \times 100\% \quad (1)$$

where HI_A is the HI of asphalt, %, G^*_0 is the initial G* of asphalt, Pa, G^*_{1-i} is the G* of asphalt after experiencing a certain modulus loss, Pa, $i = 1, 2, 3$, $G^*_{1-1} = 80\%G^*_0$, $G^*_{1-2} = 60\%G^*_0$, $G^*_{1-3} = 40\%G^*_0$, G^*_{2-i-j} is the G* of asphalt after T_j healing, Pa.

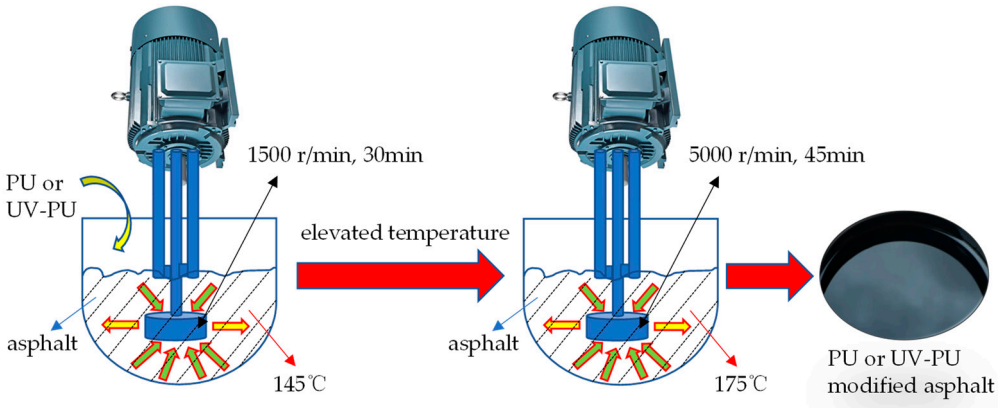


Figure 1. The preparation process PU or UV-PU modified asphalt.

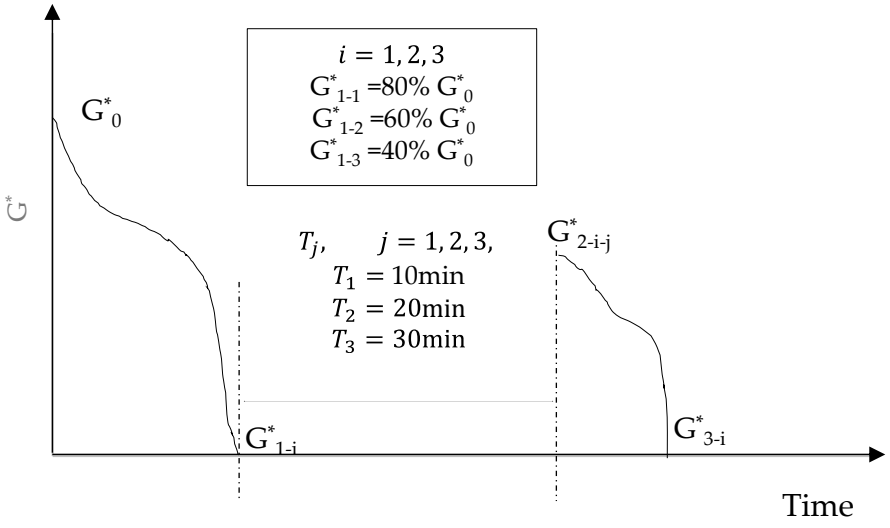


Figure 2. Asphalt self−healing test.

2.2.2. Evaluation Method and Test Design of Sand-Type Asphalt Mixture SHP

The 70#, SBS, PU, and UV-PU modified asphalt and aggregates were used to prepare sand-type asphalt mixture AC-5 rutting board, respectively. The grading of AC-5 is shown in Figure 3. After 24 h of free cooling of the rut board, the cutting machine was used to prepare a size 250 mm × 30 mm × 35 mm small beam specimen.

According to "Standard Test Methods of Bitumen and Bituminous Mixtures for Highway Engineering (JTG E20-2011)", the bending test was conducted at 15 °C, the load at which the specimen undergoes failure cracks was recorded, and the flexural tensile strength (R_{B0}) was calculated. Then turn on the fluorescent lamp to irradiate the specimen at an intensity of 27.58 W/m^2 for 1 h, 3 h, and 6 h, respectively, to promote crack healing. The fluorescent lamp simulates the full band of sunlight, including UVA (8.5%), UVB (0.2%), visible light (43%), and infrared light (48.3%). Then repeat the low-temperature bending test to obtain the load at which the failure crack occurs again and calculate the flexural tensile

strength (R_{B1-i}), as shown in Figure 4, and evaluate the healing of the asphalt according to Equations (2)–(4).

$$R_{B0} = \frac{3 \times L \times P_{B0}}{2 \times b \times h^2} \tag{2}$$

$$R_{B1-i} = \frac{3 \times L \times P_{B0-i}}{2 \times b \times h^2} \tag{3}$$

$$HI_{AC\text{-}5} = \frac{R_{B1-i}}{R_{B0}} \times 100\% \tag{4}$$

where $HI_{AC\text{-}5}$ is the HI of AC-5, %, R_{B0} is the bending tensile strength at failure of AC-5, MPa, R_{B1-i} is the flexural tensile strength when it is re lossd after T_i time (T_i, $i = 1, 2, 3$, $T_1 = 1h$, $T_2 = 3h$, $T_3 = 6h$,) of healing, MPa, P_{B0} is the maximum load at which the specimen fails, N, P_{B0-i} is the maximum load at which failure occurs again after T_i-time healing, N, b is the width of the mid-span section of the specimen, mm; h is the mid-span height of the specimen, mm; L is the span of the specimen, mm.

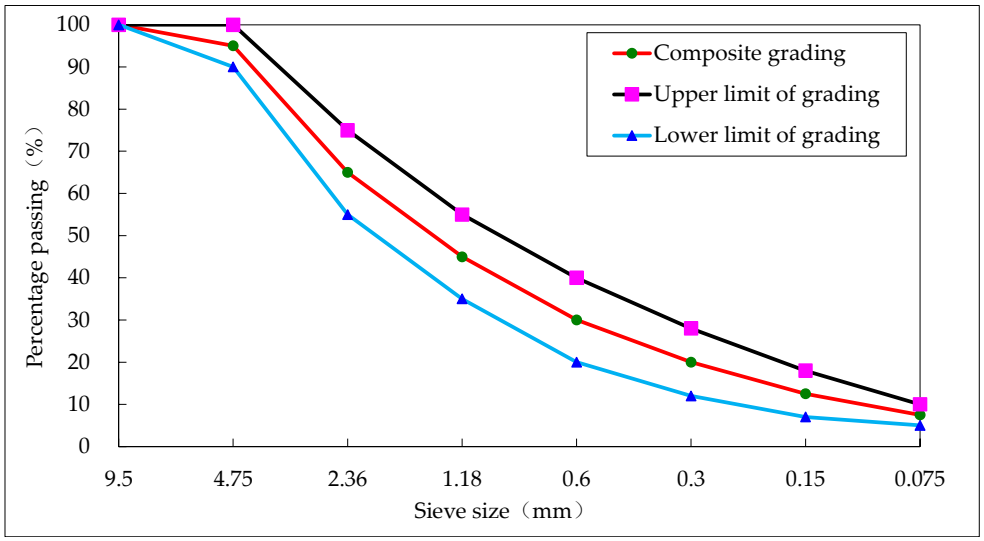


Figure 3. The grading of AC-5.

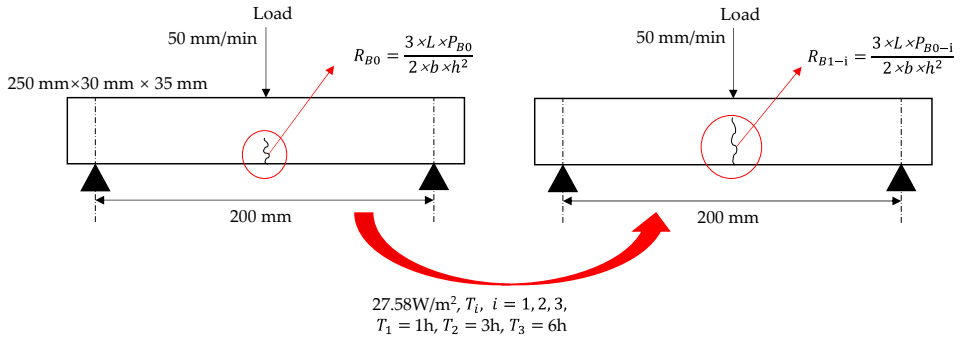


Figure 4. AC-5 self-healing test.

2.2.3. Evaluation Method and Test Design of Medium Grained Asphalt Mixture SHP

The 70#, SBS, PU, and UV-PU modified asphalt and aggregates were used to prepare sand-type asphalt mixture AC-16 rutting board, respectively. The grading of AC-16 is shown in Figure 5. After 24 h of free cooling of the rut board, the cutting machine was used to prepare a size 380 mm × 50 mm × 63 mm small beam specimen.

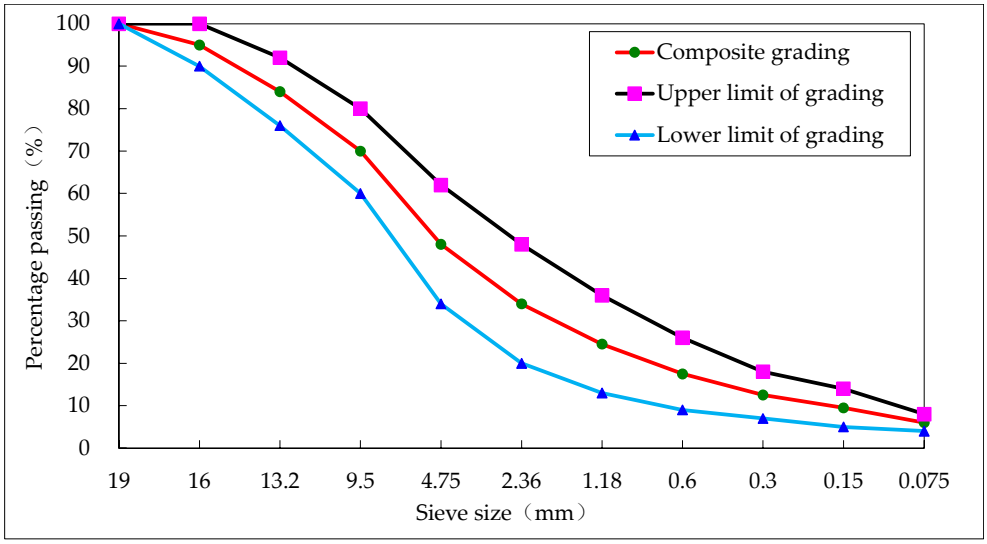


Figure 5. The grading of AC-16.

Four point bending fatigue test was conducted on AC-16 small beam specimens at 15 °C, with a controlled strain of 500 × 10^{-6}, loading frequency 10 Hz. Stop the test when the loss of stiffness modulus (S) reaches 20%, 40%, and 60%, respectively. Then turn on the fluorescent lamp to irradiate the specimen at an intensity of 27.58 W/m^2 for 8 h, 16 h, and 24 h, respectively, to promote crack healing. Then conduct the bending fatigue loading test again to test its S, as shown in Figure 6, and calculate the HI according to Equation (5).

$$HI_{AC\text{-}16} = \frac{S_{t2-i} - S_{t1-i}}{S_{t0} - S_{t1-i}} \times 100\% \quad (5)$$

where $HI_{AC\text{-}16}$ is the HI of AC-16, S_{t0} is the reference S of AC-16, Pa, S_{t1-i} is the preset S after loss, Pa, $i = 1, 2, 3$, $S_{t1-1} = 80\%S_{t0}$, $S_{t1-2} = 60\%S_{t0}$, $S_{t1-3} = 40\%S_{t0}$, S_{t2-i-j} the S when it is re lossd after T_j time (T_j, $j = 1, 2, 3$, $T_1 = 8h$, $T_2 = 16h$, $T_3 = 24h$,) of healing, Pa, σ_{t0}, σ_{t1-i}, σ_{t2-i-j} are the maximum tensile stresses under corresponding conditions, respectively, N, ε_{t0}, ε_{t1-i}, ε_{t2-i-j} are the maximum tensile strains, m/m.

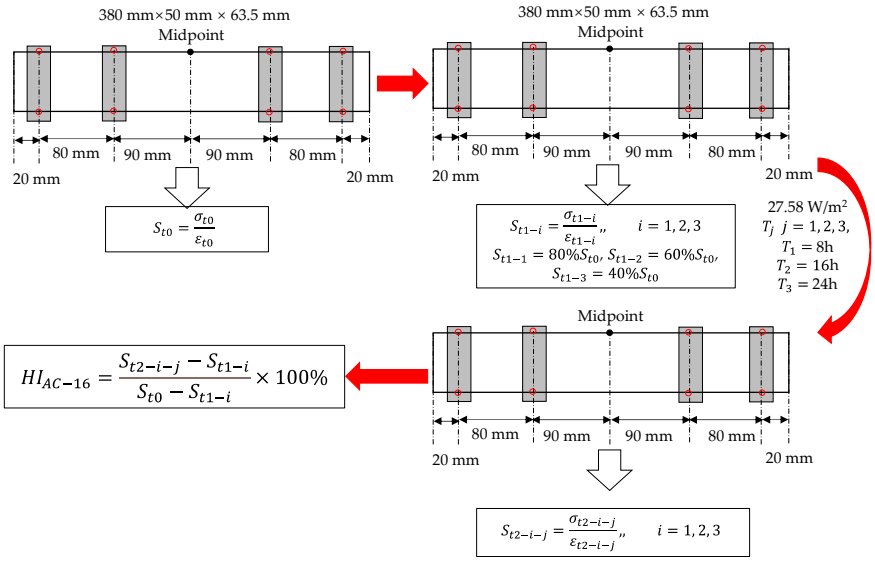


Figure 6. AC-16 self-healing test.

3. Self-Healing Performance

3.1. SHP of Asphalt

The PU and UV-PU modified asphalt with a content of 5% were prepared. Different types of asphalt were conducted DSR time scans. Due to the inability to apply light to the asphalt during the DSR test, only the asphalt type and the healing time are analyzed in the testing of asphalt healing performance. Figure 7 shows the test results of asphalt with a 20% loss of G* under different asphalt types and healing times.

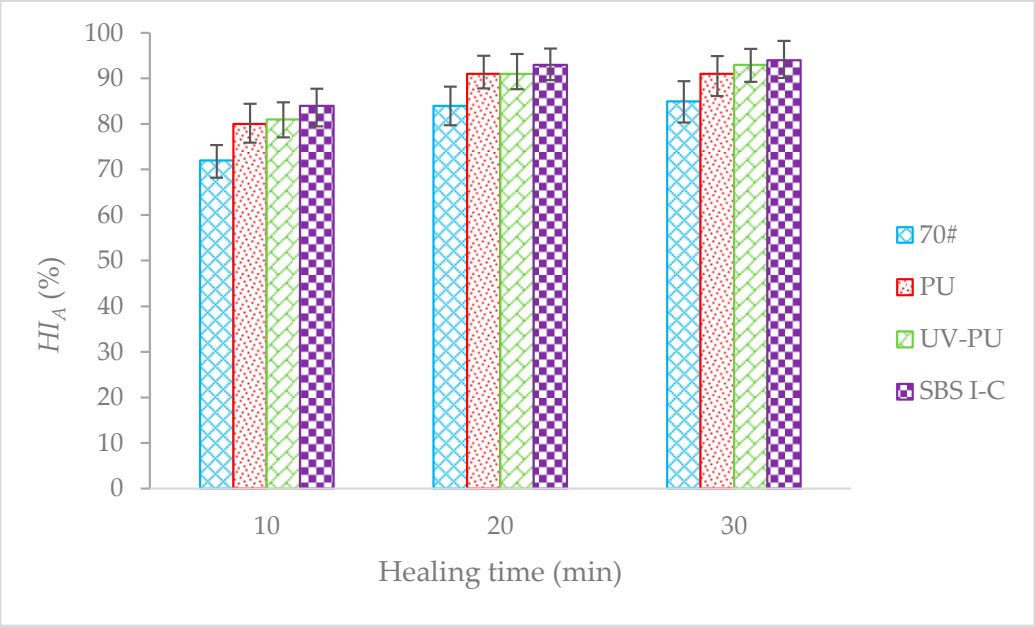


Figure 7. HI under 20% loss of G*.

The PU or UV-PU modified asphalt with a content of 5% were prepared. Different types of asphalt were conducted DSR time scans. Due to the inability to apply light to the asphalt during the DSR test, only the type of asphalt and the healing time are analyzed in the testing of asphalt healing performance. Figure 7 shows the test results of asphalt with a 20% loss of G* under different asphalt types and healing times.

Figure 7 shows that when a 20% loss in the G*, after a certain period of healing, the G* of asphalt has been restored, and with the extension of healing time, the HI first increases and then tends to stabilize. The HI of the same type of asphalt is similar when the healing time is 20 min and 30 min. For the different types of asphalt, there is a certain difference in the HI under the same healing time. When using the HI as an evaluation index to evaluate the asphalt SHP, asphalt SHP of varies from large to small, SBS I-C-modified asphalt > PU modified asphalt ≈ UV-PU modified asphalt >70$^{\#}$ asphalt.

The test results of asphalt G* loss of 40% under different types of asphalt and different healing times are shown in Figure 8.

Figure 8 shows that when a 40% loss in the G* of asphalt, after a certain period of healing, the asphalt G* can still be restored. However, compared to a preset loss of 20%, the HI of various types of asphalt has significantly decreased, and the HI of the same asphalt at 20 and 30 min of healing time is still similar. The healing indices of SBS I-C, PU or UV-PU modified asphalt is basically at the same level at the same healing time. When using the HI as an evaluation index to evaluate the asphalt SHP, the SHP of asphalt varies from large to small, SBS I-C-modified asphalt ≈ PU modified asphalt ≈ UV-PU modified asphalt >70$^{\#}$ asphalt.

The test results of asphalt G* loss of 60% under different types of asphalt and different healing times are shown in Figure 9.

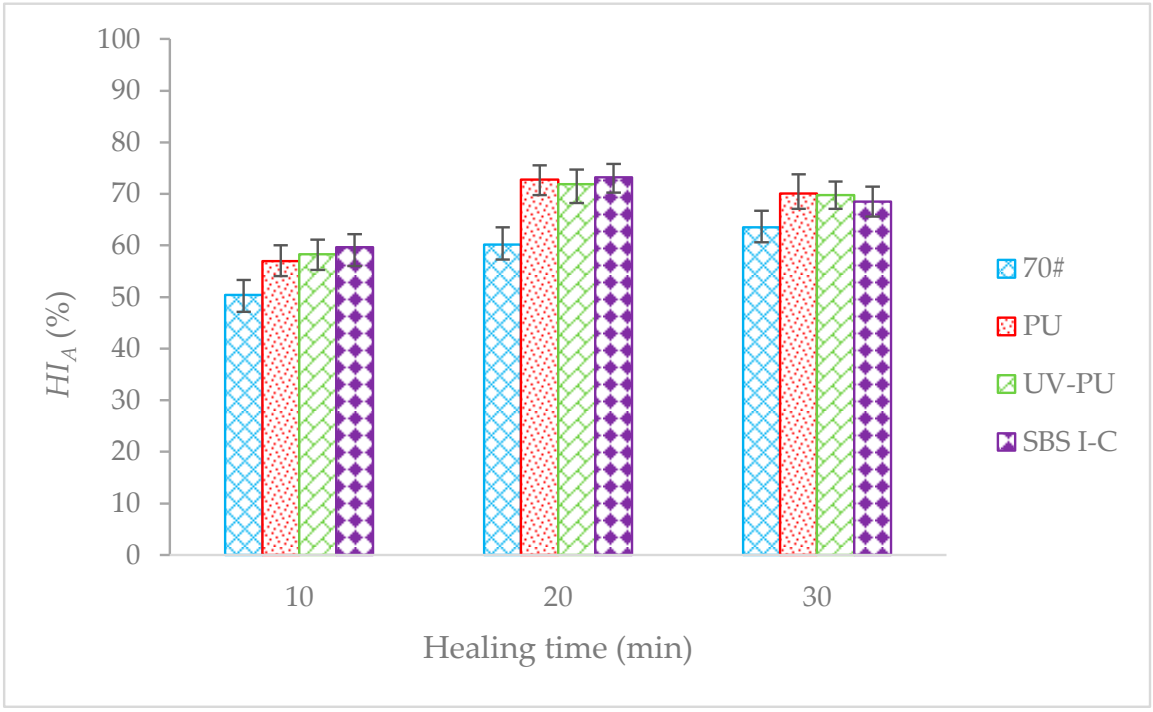


Figure 8. HI under 40% loss of G*.

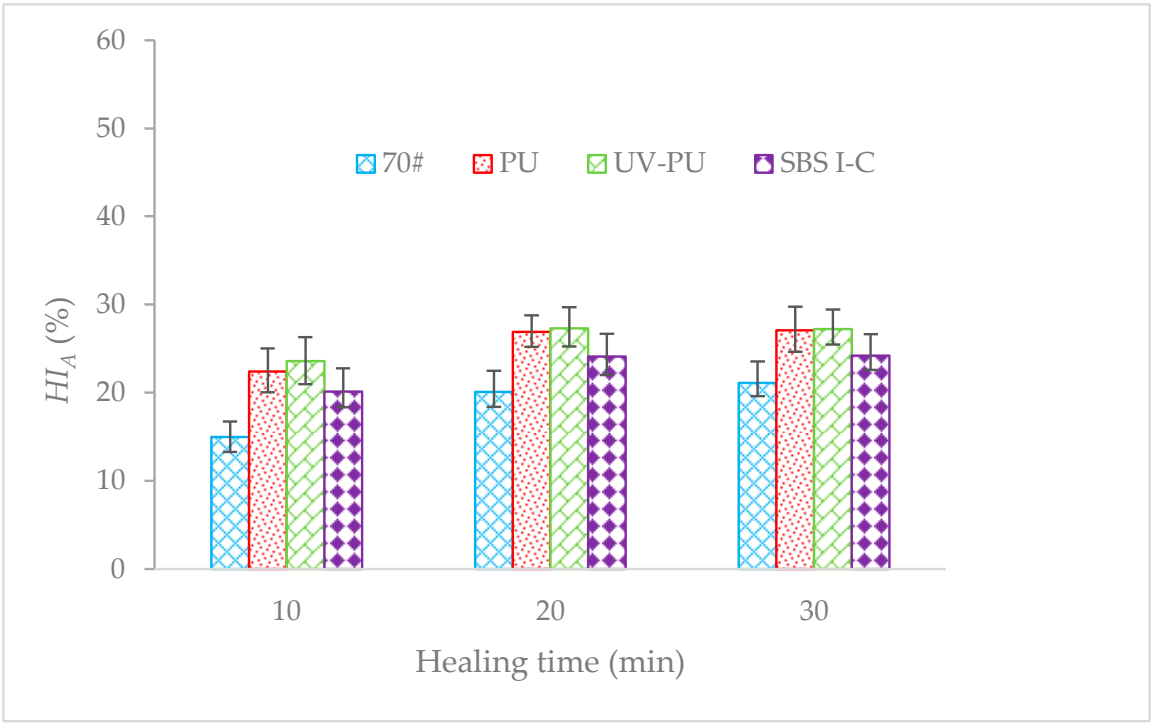
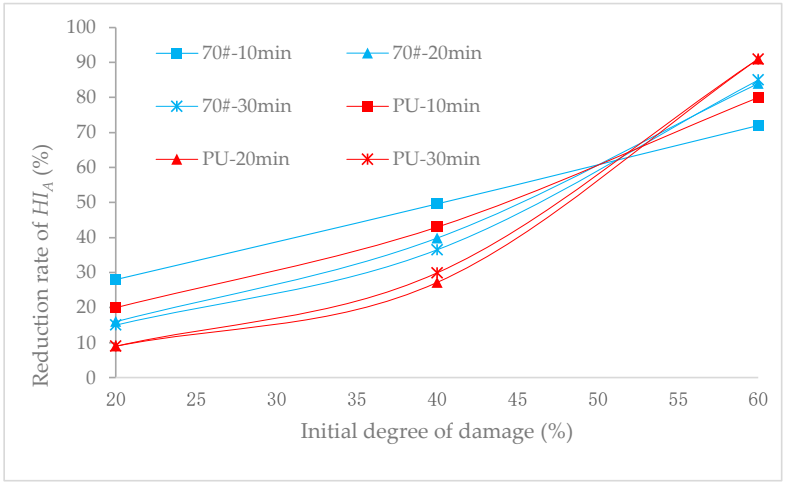


Figure 9. HI under 60% loss of G*.

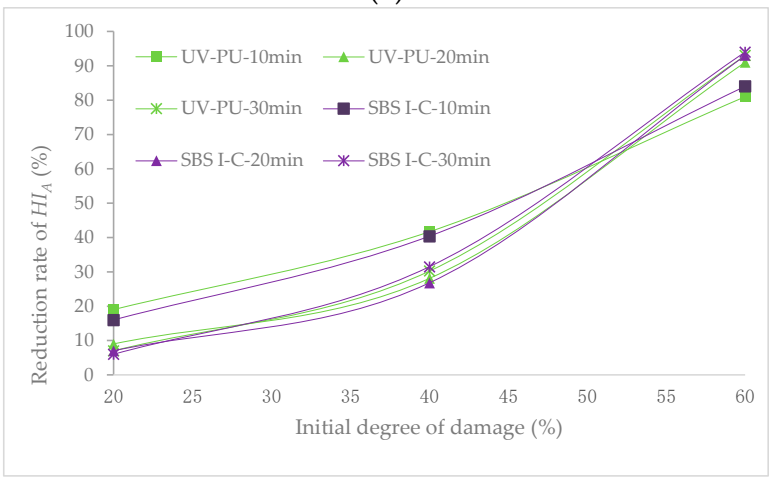
Figure 9 shows that when the G* of asphalt is lost by 60%, the healing performance of the G* of asphalt significantly decreases, and the HI of the same asphalt at healing times of 20 and 30 min is still similar. The healing performance of SBS I-C is significantly lower than that of PU or UV-PU modified asphalt, but still higher than that of 70$^{\#}$ asphalt. When using the HI as an evaluation index to evaluate the asphalt SHP, the asphalt SHP varies from large to small, PU modified asphalt ≈ UV-PU modified asphalt > SBS I-C-modified asphalt >70$^{\#}$ asphalt. PU or UV-PU additives didn't change the chemical structure of virgin

asphalt. The modification effect on asphalt can be attributed to the two-phase structure of the PU or UV-PU molecular chain. The significant improvement in the elastic recovery performance of asphalt is the reason why the self-healing performance of PU or UV-PU modified asphalt exceeds that of SBS I-C-modified asphalt under specific conditions [31].

The temperature and lighting conditions definitely have an impact on the healing performance. In this paper, in order to avoid the impact of temperature and lighting conditions changes on the research results, a method of controlling temperature and lighting conditions was adopted for the same type of material. The phenomenon indicates that without the influence of external light, and temperature changes, the SHP of asphalt is related to the asphalt type and the degree of initial loss and is highly correlated with the healing time. It can be seen from the sample in this paper that when the healing time reaches 20 min, asphalt with different types and initial complex shear modulus loss all reach the maximum HI. The greater the degree of initial G* loss, the smaller the HI of asphalt. To explore the relationship between the degree of initial G* loss and the SHP of asphalt more clearly, this paper proposes the concept of HI loss rate and establishes a relationship curve between the degree of G* loss and the HI loss rate based on test results, as shown in Figure 10.



(**a**)



(**b**)

Figure 10. Relationship between HI loss and initial loss degree, (**a**) 70# asphalt and PU modified asphalt; (**b**) UV-PU modified asphalt and SBS I-C modified asphalt.

Figure 10 clearly shows the influence of the initial loss degree of complex shear modulus on the HI loss rate. As the initial loss degree increases, the HI loss rate rapidly increases. When the initial loss degree is 20%, the HI loss rate of various types of asphalt

with different healing times ranges from 5% to 30%. This range reaches 20–50% when the initial loss level reaches 40%, and surges to 60–90% when the initial loss level reaches 60%. Compared to other asphalt types, 70# asphalt has the least sensitivity to the initial loss degree, and SBS I-C-modified asphalt has the highest sensitivity to initial loss among the tested asphalt types.

3.2. AC-5 SHP

This article selects AC-5 as the representative structure of a sand-type asphalt mixture. The different types of asphalt and aggregates were used to prepare sand-type asphalt mixture AC-5 small beam specimen. A low temperature bending test was conducted on the specimen. During this period, a fluorescent lamp was used, and the specimen was irradiated at 27.58 W/m^2 for 1 h, 3 h, and 6 h to promote crack healing. The HI of AC-5 was tested and calculated. Figure 11 shows the test results.

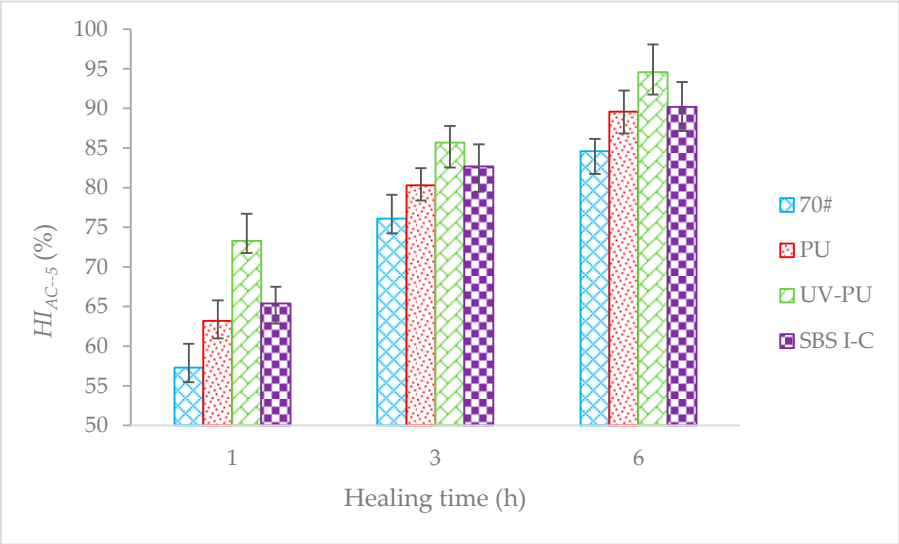


Figure 11. HI of AC-5.

Figure 11 shows that under the same light healing time, there is a significant difference in the HI of different types of AC-5, AC-5 with UV-PU modified asphalt significantly superior to other AC-5 types. When using the HI as an evaluation index to evaluate the SHP of AC-5, the SHP of AC-5 varies from large to small, UV-PU modified asphalt AC-5 > PU modified asphalt AC-5 ≈ SBS I-C-modified asphalt AC-5 > 70# asphalt AC-5. The outstanding SHP of AC-5 with UV-PU modified asphalt indicates that UV-PU modifiers play a certain role under the action of light. The mechanism is that the fluorescent lamp contains 8.5% UVA and 0.2% UVB. Under the action of these ultraviolet lights, the chitosan ring inside the UV-PU will open and generate free radicals, which can bond with the free radicals generated during loss to achieve self-healing.

In addition, AC-5 self-healing requires more time compared to asphalt. During the test, it was found that within 6 h of light self-healing, the HI of AC-5 significantly increased with the prolongation of healing time. The HI of AC-5 prepared with different asphalt types (UV-PU, PU, SBS I-C and 70#) at 1 h healing time were only 73.3%, 63.2%, 65.4%, and 57.3%, while these values increased to 94.6%, 89.6%, 90.2%, and 84.1% at 6 h healing time. This phenomenon suggests that sufficient healing time is the basic guarantee for the healing effect after the appearance of microcracks in AC-5.

3.3. AC-16 SHP

This article selects AC-16 as the representative structure of a medium grained asphalt mixture. The different types of asphalt and aggregates were used to prepare sand-type asphalt mixture AC-16 small beam specimen. Four-point bending fatigue testing was

constructed on AC-16 small beam specimens. The 20% loss of S (S) was used as the test reference condition, and specimens were irradiated with a fluorescent lamp with an irradiation intensity of 27.58 W/m^2 for 8 h, 16 h, and 24 h to promote healing. Then, a bending fatigue loading test was conducted again to test and calculate the HI of AC-16. The test results are summarized in Figure 12.

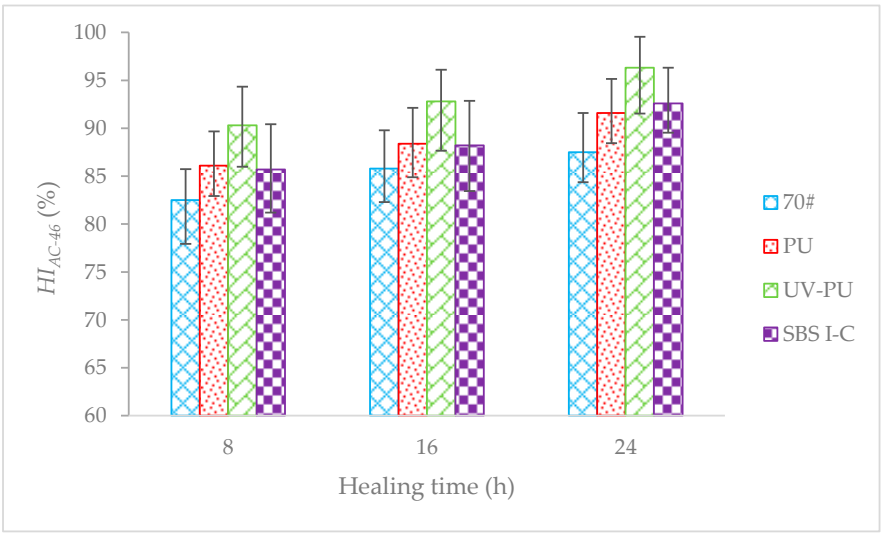


Figure 12. HI under 20% S loss (AC-16).

Figure 12 shows that at a 20% initial S loss level, after a certain healing time, the S of AC-16 shows a certain recovery. When it is reflected in the HI, it shows an increase in numerical value, and the longer the healing time, the greater the HI. With the action of the self-healing function of UV-PU Under ultraviolet light, at the same healing time, UV-PU modified asphalt mixture has the highest HI. When using the HI as an evaluation index to evaluate the SHP of AC-16, the SHP of AC-16 varies from large to small, UV-PU modified asphalt AC-5 > PU modified asphalt AC-5 ≈ SBS I-C modified asphalt AC-5 > 70$^{\#}$ asphalt AC-5.

The 40% loss of S was used as the test reference condition, and specimens were irradiated with a fluorescent lamp with an irradiation intensity of 27.58 W/m^2 for 8 h, 16 h, and 24 h to promote healing. Then, a bending fatigue loading test was conducted again to test and calculate the HI of AC-16. Figure 13 shows test results.

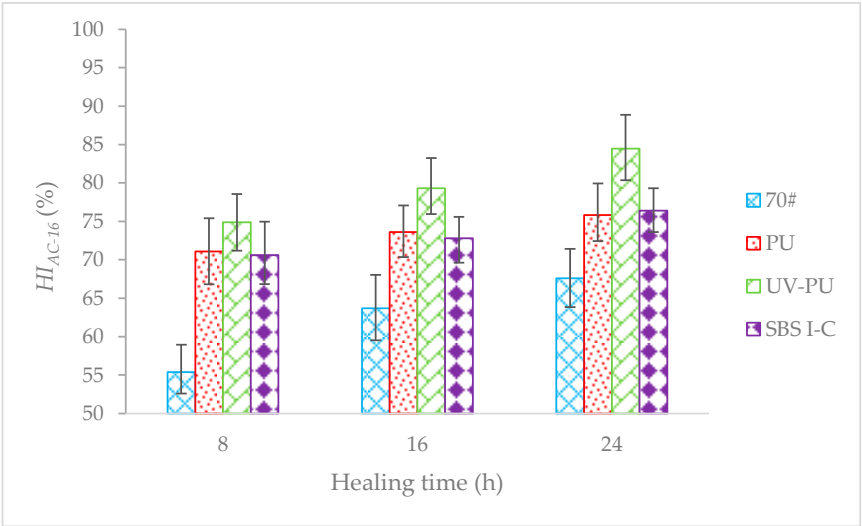


Figure 13. HI under 40% S loss (AC-16).

Figure 13 shows that at a 40% initial S loss level, the HI of various asphalt mixtures shows a significant decrease compared to a 20% initial S loss. However, after a certain healing time, their S still shows some recovery. The advantage of the UV-PU modified asphalt mixture HI is significant, and its value can still be maintained at around 85% after 24 h of healing time. In addition, the other rules are similar to the initial S of 20% and will not be repeated.

The 60% loss of S was used as the test reference condition, and specimens were irradiated with a fluorescent lamp with an irradiation intensity of 27.58 W/m^2 for 8 h, 16 h, and 24 h to promote healing. Then, a bending fatigue loading test was conducted again to test and calculate the HI of AC-16. Figure 14 shows test results.

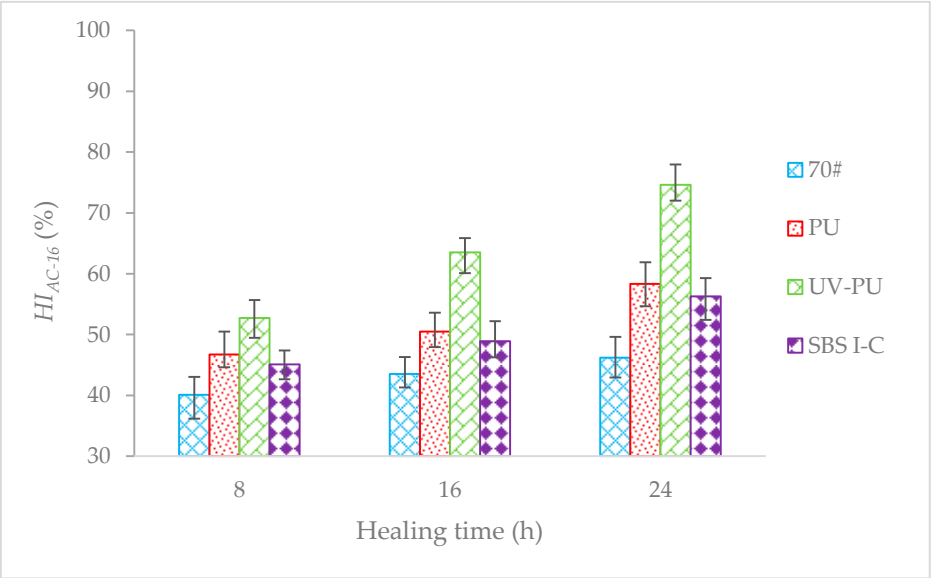
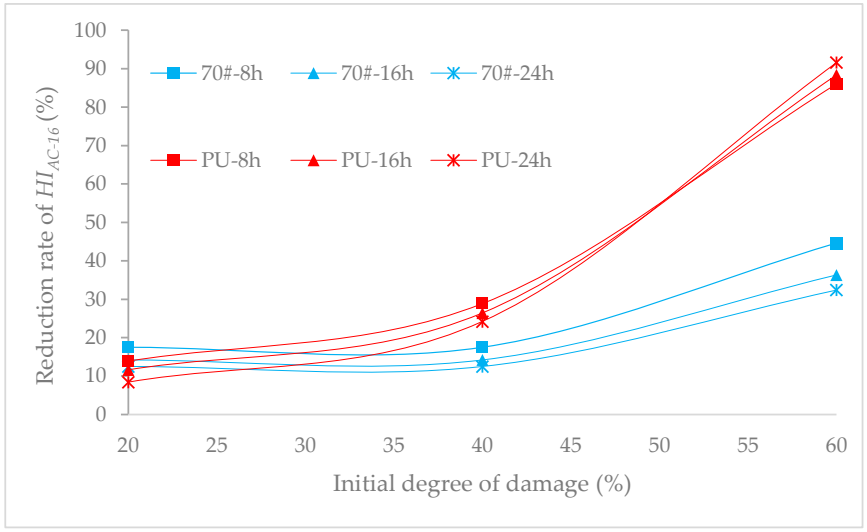


Figure 14. HI under 60% S loss (AC-16).

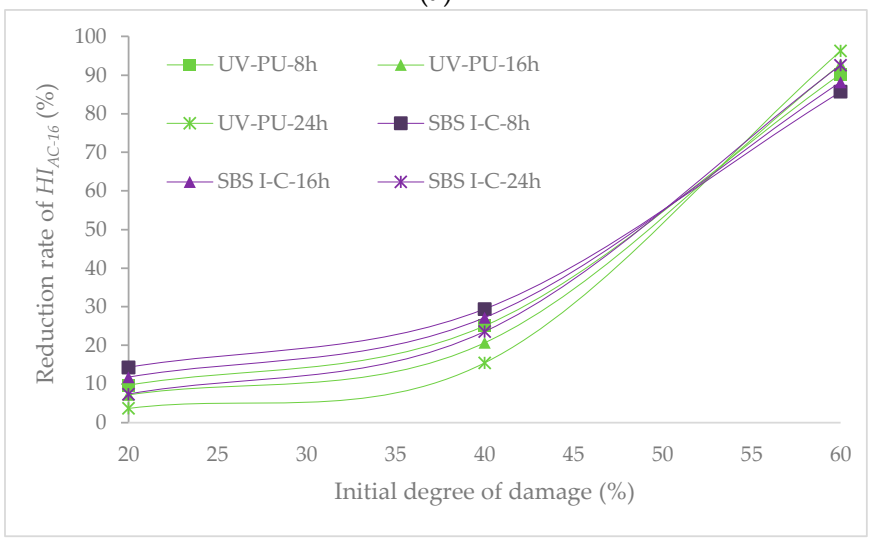
Figure 14 shows that at the initial S loss level of 60%, the HI of various asphalt mixtures decreases significantly compared to the initial S loss levels of 20% and 40%. After a certain healing time, the advantage of UV-PU modified asphalt mixture HI is significant, and the HI of PU modified asphalt mixture is higher than that of the SBS I-C at each healing time. When using the HI as an evaluation index to evaluate the SHP of AC-16, the SHP of AC-16 varies from large to small, UV-PU modified asphalt AC-5 > PU modified asphalt AC-5 > SBS I-C modified asphalt AC-5 > 70$^{\#}$ asphalt AC-5.

This phenomenon indicates that the SHP of asphalt mixtures is related to the asphalt mixture types and the healing time, and is highly correlated with the degree of loss to the initial S. In order to explore the relationship between the degree of the initial S loss and the SHP of asphalt mixtures more clearly, this paper establishes a relationship curve between the degree of the initial S loss and the self-HI loss rate based on the concept of HI loss rate, as shown in Figure 15.

Figure 15 clearly shows the relationship between initial S loss and HI loss rate. As the initial S loss increases, the loss rate of the HI rapidly increases. When the initial loss is 20%, the HI loss rate of various types of asphalt mixture with different healing times ranges from 5% to 20%. This range reaches 10–30% when the initial loss reaches 40%, and surges to 80–90% when the initial loss reaches 60%. However, the 70$^{\#}$ asphalt mixture is relatively special. From the test results, it is not sensitive to the initial loss, and the highest HI loss rate does not exceed 40%, which is far lower than other asphalt mixture types. The other three asphalt mixture types show similar performance.



(**a**)



(**b**)

Figure 15. The relationship between the loss of AC-16 HI and the degree of initial S loss, (**a**) 70# asphalt mixture and PU modified asphalt mixture, (**b**) UV-PU modified asphalt mixture and SBS I-C modified asphalt mixture.

4. Conclusions

This paper conducted research on the evaluation method and influence factor of the SHP of UV-PU modified asphalt and asphalt mixtures. To make the research comparable, PU, SBS I-C and 70# asphalt and asphalt mixtures were introduced as the example of comparison. A method for evaluating the asphalt SHP, sand asphalt mixture, and medium particle asphalt mixture using the HI as an evaluation index was proposed, and the healing performance of various materials under different healing conditions was tested and analyzed.

(1) HI based on asphalt complex shear modulus (HI_A), HI based on sand type asphalt mixture (AC-5) flexural tensile strength ($HI_{AC\text{-}5}$), and HI based on medium grained asphalt mixture (AC-16) S $HI_{AC\text{-}16}$ can effectively reflect the SHP of asphalt, AC-5, and AC-16 under different healing conditions, and can be used as an evaluation indicator for SHP.

(2) Without the influence of external light, and temperature changes, the SHP is related to the type of asphalt and the degree of initial damage and is highly correlated with

the healing time. The asphalt with different types and initial complex shear modulus loss all reach the maximum HI when the healing time reaches 20 min.

(3) The greater the initial loss of asphalt's initial G*, the faster the loss rate of the HI increases. Compared to other types of asphalt, the sensitivity of UV-PU modified asphalt and PU modified asphalt to initial loss is lower than that of SBS I-C modified asphalt, but higher than 70# asphalt.

(4) Under the same light healing time and initial degree of loss, the SHP of UV-PU modified asphalt AC-5 and AC-16 is significantly superior to other types of asphalt mixtures. Compared to asphalt, the self-healing time of AC-5 grade AC-16 is much longer.

(5) The AC-16 SHP is highly correlated with the initial S loss. The larger the initial loss degree of the S, the greater the loss rate of the HI.

Author Contributions: Conceptualization, J.Z. and W.Z.; Data curation, X.C. and D.W.; Formal analysis, W.L. and S.S.; Funding acquisition, Y.W. and W.Z.; Investigation, Y.W. and J.Z.; Methodology, H.S. and W.Z.; Project administration, W.Z.; Resources, W.L.; Software, H.S., X.C. and S.S.; Supervision, H.Z. and J.X.; Visualization, H.Z.; Writing—original draft, H.S. and W.Z.; writing—review and editing, J.X. and W.Z. All authors have read and agreed to the published version of the manuscript.

Funding: This research was funded by Technology Development Projects of Tianjin South Railway Station Technology Business District Development Co., Ltd., China, grant number 9101/2230071; Key Laboratory of Transport Industry of Road Structure and Material Research Institute of Highway, Ministry of Transport), China, grant number 2019-Keji-271.

Institutional Review Board Statement: Not applicable.

Informed Consent Statement: Not applicable.

Data Availability Statement: Not applicable.

Acknowledgments: Many thanks for the equipment support provided by Tianjin Municipal Engineering Design and Research Institute.

Conflicts of Interest: The authors declare no conflict of interest.

References

1. Garcia, A.; Schlangen, E.; Van de Ven, M. Two ways of closing cracks on asphalt concrete pavements: Microcapsules and induction heating. In *Key Engineering Materials*; Trans Tech Publications Ltd.: Zurich, Switzerland, 2010; Volume 417, pp. 573–576. [CrossRef]
2. Wang, L.; Wang, H.; Zhao, Q.; Yang, H. Development and prospect of intelligent pavement. *China J. Highw. Transp.* **2019**, *4*, 50–72. [CrossRef]
3. Zhang, W.; Qiu, L.; Liu, J.; Hu, K.; Zou, L.; Chen, Y.; Yang, C.; Wang, F.; Zang, J. Modification mechanism of C9 petroleum resin and its influence on SBS modified asphalt. *Constr. Build. Mater.* **2021**, *306*, 124740. [CrossRef]
4. Liang, B.; Lan, F.; Shi, K.; Qian, G.; Zheng, J. Review on the self-healing of asphalt materials: Mechanism, affecting factors, assessments and improvements. *Constr. Build. Mater.* **2021**, *266*, 120453. [CrossRef]
5. Anupam, B.R.; Sahoo, U.C.; Chandrappa, A.K. A methodological review on self-healing asphalt pavements. *Constr. Build. Mater.* **2022**, *321*, 126395. [CrossRef]
6. Li, Y.; Hao, P.; Zhang, M. Fabrication, characterization and assessment of the capsules containing rejuvenator for improving the self-healing performance of asphalt materials: A review. *J. Clean. Prod.* **2021**, *287*, 125079. [CrossRef]
7. He, L.; Li, G.; Lv, S.; Gao, J.; Kowalski, K.J.; Valentin, J.; Alexiadis, A. Self-healing behavior of asphalt system based on molecular dynamics simulation. *Constr. Build. Mater.* **2020**, *254*, 119225. [CrossRef]
8. Ruiz-Riancho, N.; Garcia, A.; Grossegger, D.; Saadoon, T.; Hudson-Griffiths, R. Properties of Ca-alginate capsules to maximise asphalt self-healing properties. *Constr. Build. Mater.* **2021**, *284*, 122728. [CrossRef]
9. Lyu, L.; Li, D.; Chen, Y.; Tian, Y.; Pei, J. Dynamic chemistry based self-healing of asphalt modified by diselenide-crosslinked polyurethane elastomer. *Constr. Build. Mater.* **2021**, *293*, 123480. [CrossRef]
10. Liu, K.; Xu, P.; Wang, F.; You, L.; Zhang, X.; Fu, C. Assessment of automatic induction self-healing treatment applied to steel deck asphalt pavement. *Autom. Constr.* **2022**, *133*, 104011. [CrossRef]
11. Cong, L.; Yang, F.; Guo, G.; Ren, M.; Shi, J.; Tan, L. The use of polyurethane for asphalt pavement engineering applications: A state-of-the-art review. *Constr. Build. Mater.* **2019**, *225*, 1012–1025. [CrossRef]
12. Huang, G.; Yang, T.; He, Z.; Yu, L.; Xiao, H. Polyurethane as a modifier for road asphalt: A literature review. *Constr. Build. Mater.* **2022**, *356*, 129058. [CrossRef]

13. Wang, C.; Huang, S.; Chen, Q.; Ji, X.; Duan, K. Materials, preparation, performances and mechanism of polyurethane modified asphalt and its mixture: A systematic review. *J. Road Eng.* **2023**, *3*, 16–34. [CrossRef]
14. Liu, H.; Zhang, Z.; Zhu, Y.; Sun, J.; Wang, L.; Huang, T.; Chen, L. Modification of asphalt using polyurethanes synthesized with different isocyanates. *Constr. Build. Mater.* **2022**, *327*, 126959. [CrossRef]
15. Zhang, Z.; Sun, J.; Huang, Z.; Wang, F.; Jia, M.; Lv, W.; Ye, J. A laboratory study of epoxy/polyurethane modified asphalt binders and mixtures suitable for flexible bridge deck pavement. *Constr. Build. Mater.* **2021**, *274*, 122084. [CrossRef]
16. Jia, M.; Zhang, Z.; Yang, N.; Qi, B.; Wang, W.; Huang, Z.; Sun, J.; Luo, F.; Huang, T. Performance Evaluation of Thermosetting and Thermoplastic Polyurethane Asphalt Mixtures. *J. Mater. Civ. Eng.* **2022**, *34*, 04022097. [CrossRef]
17. Zhao, Y.; Chen, M.; Wu, S.; Jiang, Q.; Xu, H.; Zhao, Z.; Lv, Y. Effects of waterborne polyurethane on storage stability, rheological properties, and VOCs emission of crumb rubber modified asphalt. *J. Clean. Prod.* **2022**, *340*, 130682. [CrossRef]
18. Jin, X.; Guo, N.; You, Z.; Wang, L.; Wen, Y.; Tan, Y. Rheological properties and micro-characteristics of polyurethane composite modified asphalt. *Constr. Build. Mater.* **2020**, *234*, 117395. [CrossRef]
19. Chen, B.; Dong, F.; Yu, X.; Zheng, C. Evaluation of properties and micro-characteristics of waste polyurethane/styrene-butadiene-styrene composite modified asphalt. *Polymers* **2021**, *13*, 2249. [CrossRef]
20. Zhang, Z.; Sun, J.; Jia, M.; Ban, X.; Wang, L.; Chen, L.; Huang, T.; Liu, H. Effects of polyurethane thermoplastic elastomer on properties of asphalt binder and asphalt mixture. *J. Mater. Civ. Eng.* **2021**, *33*, 04020477. [CrossRef]
21. Sha, A.; Zhang, J.; Jia, M.; Jiang, W.; Jiao, W. Development of polyurethane-based solid-solid phase change materials for cooling asphalt pavements. *Energy Build.* **2022**, *259*, 111873. [CrossRef]
22. Li, Z.; Yang, F.; Yuan, J.; Cong, L.; Yu, M. Study on preparation and pavement performance of polyurethane modified asphalt based on in-situ synthesis method. *Constr. Build. Mater.* **2021**, *309*, 125196. [CrossRef]
23. Zhang, W.; Zou, L.; Chen, F.; Yang, C.; Li, Y.; Yan, X.; Zang, J.H.; Liu, J. Evaluation method of storage stability of SBS modified bitumen based on dynamic rheological properties. *Constr. Build. Mater.* **2022**, *323*, 126615. [CrossRef]
24. Sun, J.; Zhang, Z.; Ye, J.; Liu, H.; Wei, Y.; Zhang, D.; Li, X. Preparation and properties of polyurethane/epoxy-resin modified asphalt binders and mixtures using a bio-based curing agent. *J. Clean. Prod.* **2022**, *380*, 135030. [CrossRef]
25. Li, S.; Xu, W.; Zhang, F.; Wu, H.; Zhao, P. Effect of Graphene Oxide on the Low-Temperature Crack Resistance of Polyurethane–SBS-Modified Asphalt and Asphalt Mixtures. *Polymers* **2022**, *14*, 453. [CrossRef]
26. Zhou, X.; Sun, B.; Wu, S.; Zhang, X.; Liu, Q.; Xiao, Y. Evaluation on self-healing mechanism and hydrophobic performance of asphalt modified by siloxane and polyurethane. *J. Wuhan Univ. Technol. Mater. Sci. Ed.* **2019**, *34*, 630–637. [CrossRef]
27. Jia, M.; Sha, A.; Lin, J.; Zhang, Z.; Qi, B.; Yuan, D. Polyurethane asphalt binder: A promising candidate for steel bridge deck-paving material. *Int. J. Pavement Eng.* **2022**, *23*, 3920–3929. [CrossRef]
28. Zhang, W.; Zou, L.; Wang, Y.; Liu, J.; Yang, C.; Di, J.; Hu, H.; Yang, Z. Influence of High Viscosity Petroleum Resin (HV-PR) on the Intermediate and High Temperature Performances of Styrene-Butadiene-Styrene Block Copolymer (SBS) Modified Bitumen. *Arab. J. Sci. Eng.* **2022**, *47*, 12521–12533. [CrossRef]
29. Jia, P.; Ji, X.; Zheng, B.; Wang, C.; Hao, W.; Han, W.; Zhang, J.; Xia, G.; Ji, X.; Zhang, J. Eco-Friendly and Complete Recycling of Waste Bamboo-Based Disposable Paper Cups for Value-Added Transparent Cellulose-Based Films and Paper Plastic Composites. *Polymers* **2022**, *14*, 1589. [CrossRef]
30. Research Institute of Highway Ministry of Transport. *Standard Test Methods of Bitumen and Bituminous Mixtures for Highway Engineering (JTG E20-2011)*; China Communications Press: Beijing, China, 2011; pp. 249–253. (In Chinese)
31. Zhao, Y.; Gong, X.; Liu, Q. Research on rheological properties and modification mechanism of waterborne polyurethane modified bitumen. *Constr. Build. Mater.* **2023**, *371*, 130775. [CrossRef]

Disclaimer/Publisher's Note: The statements, opinions and data contained in all publications are solely those of the individual author(s) and contributor(s) and not of MDPI and/or the editor(s). MDPI and/or the editor(s) disclaim responsibility for any injury to people or property resulting from any ideas, methods, instructions or products referred to in the content.